RSC Advances

ROYAL SOCIETY OF CHEMISTRY

www.rsc.org/advances

Journal Name

ARTICLE

Three-Dimensional Potassium Niobate Nanoarray on Vermiculite for High-performance Photocatalyst Fabricated by an *in situ* Hydrothermal process

Received 00th January 20xx,
Accepted 00th January 20xx

DOI: 10.1039/x0xx00000x

www.rsc.org/

Yuwei Wang, [a] Xianggui Kong, [a,*] Weiliang Tian,[a] Deqiang Lei [b] and Xiaodong Lei [a,*]

Abstract: The three-dimensinal (3D) potassium niobate nanoarray/vermiculite ($KNbO_3$/VMT) was synthesized by an *in situ* hydrothermal method using niobium chloride as niobium resource. Scanning electron microscopy, high resolution transmission electron microscopy, X-ray diffraction, Fourier transform infrared and X-ray photoelectron spectroscopy tests were used to confirm that $KNbO_3$ nanoneedles have been grown both on the outer and inner surfaces of natural layered VMT and the growth mechanism of well aligned $KNbO_3$ nanoarray grown on mineral VMT was attributed to the existence of Nb species. The photocatalytic performance of the as-prepared composite was investigated by using the photodegradation of methylene blue（MB） under illumination. The MB was removed from aqueous slution by fully taking advantage of the good absorption property of VMT and photocatalytic property of $KNbO_3$, and visible light was used in the process. After illumination for 105 min, the removal rate of MB in aqueous solution could be higher than 81%. The removal of MB via adsorption-degradation synergy of the structured composite was much better than that of pristine VMT and $KNbO_3$ powder with the same amount of addition, respectively. Moreover, the environmental friendly $KNbO_3$/VMT material is facile to synthesize and expected to be a promising structured photocatalyst for removal of dyes.

1 Introduction

Currently, potassium niobate ($KNbO_3$), as a typical example of perovskite-type materials, has attracted great attention because of their excellent ferroelectric and photocatalytic properties.[1-3] Such as Au/$KNbO_3$ composite was synthesized as photocatalyst by loaded the Au nanoparticles on the surface of one-dimensional $KNbO_3$ nanowires which exhibited well photocatalytic activity under ultraviolet and visible-light illumination,[4] and the nitrogen-doped $KNbO_3$ nanocube has also been developed for enhancing its photocatalytic performance for water splitting and dye degradation.[5] However, there still exist several disadvantages in the photocatalysis process by using $KNbO_3$ powder. In general, photocatalytic particles have high activity when they are small enough to ensure a large surface area. Unfortunately, owing to the aggregation of $KNbO_3$ nanoparticles and the bad dispersion stability in aqueous solution, both effective surface area and photocatalytic efficiency of the material are largely deduced. In addition, although $KNbO_3$ possesses a wide band gap, its photoactivity only can be motivated under UV light, which accounts for only 4% of the solar energy, thus greatly limiting its practical applications.[2g,4] Furthermore, the difficulty and cost of filtration, recovery and recycling of photocatalysts in powder form also limited their application.[6] To solve above problems, considerable attention has been paid on the development of the catalyst-coated on supports to weak the separation and recycling spending and expand the photocatalytic response into visible region.

Constructing 3D architecture by supporting catalytic powder on mesoporous materials can partially solve above problems with increasing the photocatalytic activity of the active material. Compared with the powder catalyst, 3D composites retain several prominent advantages, such as large contacting surface, facilitating electron transportation, highly dispersing and reducing separation cost. Recently, a lot of attention has been focused on supporting catalytic powder on mesoporous materials in terms of their very large surface areas.[7] Among layered materials, mineral vermiculite (VMT) is a suitable candidate because it can offer large surface area, good absorbability, heat stability and reproducibility. Moreover, VMT can also absorb visible light. Besides, VMT is a natural phyllosilicate clay material with no-toxic and environmental friendly properties.[8] For example, a CdS quantum dot sensitized VMT photocatalyst was successfully prepared and exhibited good photocatalytic activity for hydrogen evolution under light irradiation.[9]

VMT is a magnesium aluminium silicate with 2:1 crystalline structure that made up by two silica tetrahedral sheets and one magnesium octahedral sheet.[10] The size of natural VMT is

[a] *State Key Laboratory of Chemical Resource Engineering, Beijing University of Chemical Technology, Beijing 100029, China.* Tel.: +86-10-64455357. Fax: +86-10-64425385. E–mail address: leixd@mail.buct.edu.cn; kongxg@mail.buct.edu.cn.
[b] *Department of Neurosurgery, Union Hospital, Tongji Medical College, Huazhong University of Science and Technology, Wuhan 430022, China.*

big enough (0.5 mm to 10 mm) which is advantageous to separation and recovery. Generally, owing to negatively charged layer of the VMT, it has presented excellent practical application as a sorbent in environmental protection for removing heavy metal from wastewater and in the treatment of oily waters by ion exchange/sorption.[11] Furthermore, a little amount of Nb species exists in the layer of VMT[12] that benefit to provide active sites where $KNbO_3$ can *in situ* growth. At the same time, based on the adsorbing characteristics of VMT, it could utilize niobium source which contains Nb^{5+} to be absorbed on the surface of VMT and *in situ* growth of $KNbO_3$ by hydrothermal synthesis. Meanwhile, $KNbO_3$ requires UV light irradiation for photocatalytic activation, while VMT has a good absorption in visible region. Inspired by the above consideration, it should be a good choice to fabricate the hybrid with 3D structure in which VMT worked as substrate for $KNbO_3$, resulting in a co-cooperation between VMT and $KNbO_3$, which should be display a better absorption in visible region range.

There are some literatures have reported about using $KNbO_3$ powder as photocatalyst,[1a,3c,4] but to the best of our knowledge, investigating about utilizing structured 3D $KNbO_3$ composite materials as photocatalysts are still few. In this work, a 3D $KNbO_3$ nanoarry/VMT composite was synthesized by a facial *in situ* hydrothermal method. The photocatalytic performance of the structured $KNbO_3$/VMT was investigated by using photocatalytic degradation of MB in water under illumination, exhibiting a well photocatalytic performance (about 81% removal rate of MB after 105 min irradiation with 0.3 g catalyst). It can be conclude that the hierarchical architecture composite in this work should be a promising photocatalyst that will practical apply in photocatalysis and relevant areas.

2 Experimental

2.1 Materials

Heat expanded natural VMT (calcined at about 1000 °C) was purchased from Xinjiang Yuli vermiculite Co. Ltd, China. The expanded VMT was immersed in alcohol（purity≥99.7%）for 24 h at room temperature, then filtrated and dried at 60 °C for 24 h prior to use. Niobium chloride ($NbCl_5$, 99%, Aladdin), potassium hydroxide (KOH, purity ≥ 85.0 %, Sinopharm Chemical Reagent Co.,Ltd), MB（purity ≥98.5%, Sinopharm Chemical Reagent Co.,Ltd), p-benzoquinone (BQ, 97%, Aladdin), isopropanol (i-PrOH, purity ≥ 99.7 %, Sinopharm Chemical Reagent Co.,Ltd) were used without any further purification. .

2.2 The fabrication of $KNbO_3$ nanoarray/VMT composite

The composite was prepared by an *in situ* hydrothermal method. 39.2 g KOH was dissolved into 30 mL deionized water with magnetic stirring. After being completely dissolved, 0.5 g VMT was added and then 1.82 g $NbCl_5$ was added slowly to the mixture in 30 min. After stirred vigorously at room temperature for 30 min, the reaction mixture was sealed in an 80 mL Teflon-lined stainless steel autoclave and heated up to 180 °C, then maintained at this temperature up to 12 h. After cooling to room temperature, the precipitate was washed several times with deionized water until the washing solution was clear and the pH of washing water was 7. At last, the precipitate was dried at 60 °C for 24 h. The obtained sample was denoted as $KNbO_3$/VMT.

For obtain powder $KNbO_3$, 39.2 g KOH was dissolved into 30 mL deionized water with magnetic stirring, 1.82 g $NbCl_5$ was added slowly into the solution after KOH is completely dissolved. Stirring the mixture at room temperature for 30 min, then sealed it into an 80 mL Teflon-lined stainless steel autoclave and heated up to 180 °C and maintained at this temperature for 12 h. After cooling to room temperature, the suspension was vacuum filtrated. The filtrated solid was washed with deionized water till the pH of washing water was about 7. $KNbO_3$ powder was obtained by dried at 60 °C for 24 h.

2.3 Characterization

The crystal structure of the as-synthesized samples were investigated by powder X-ray diffraction (XRD, Rigaku UItimaI II) in the 2θ range of 3 - 70° at a scanning step of 10^o min^{-1}. Fourier transform infrared (FTIR) spectra were performed on a Nicolet 380 instrument between 4000 and 400 cm^{-1}. Scanning electron microscopy (SEM) data were collected with ZEISS Supra 55 to explore the morphology of the as-synthesized samples. The energy dispersed X-ray spectroscopy (EDX) was used to determine the $KNbO_3$ loadings. High resolution transmission electron microscopy (HRTEM) images were obtained using a JEM 2100-HRTEM microscope operating at 200 kV. X-ray photoelectron spectroscopy (XPS) data were obtained by using an ESCALAB 250 electron spectrometer from Thermo Scientific Corporation. A monochromatic 150 W Al Kα source with a passing energy of 30 eV was used to get the high-resolution spectra. Low-energy electrons were utilized to compensate charge. The binding energies were relative to the adventitious C1s line at 284.8 eV. Diffuse reflectance ultraviolet and visible (DRUV-vis) spectra were obtained on a Tsushima UV-3600 UV-vis spectrometer in the range of 200–700 nm. The standard was fine $BaSO_4$ powder. The loading amount of $KNbO_3$ on VMT was determined by the Inductively Coupled Plasma (ICP) test on a Shinadzu ICPS-7500 instrument on solutions prepared by dissolving the samples in HCl with HNO_3 solution (volume ratio of concentrated hydrochloric acid *vs* nitric acid solution was 3:1) for 24 h. Photoluminescence (PL) spectra were recorded using a CanyECLIPSe fluorescence spectrophotometer (Varian, USA) with an excitation at 260 nm light. Nitrogen adsorption–desorption measurements were conducted on a Conta AS-1C-VP analyzer. Samples were outgassed at 373 K for 6 h. The specific surface areas were calculated using the Brunauer-Emmett-Teller (BET) method based on the N_2 adsorption isotherms.

2.4 Photocatalysis testing

The photocatalytic performance of $KNbO_3$/VMT composite was evaluated by degrading MB under irradiation in aqueous solutions. Prior to irradiation, 0.3 g $KNbO_3$/VMT was mixed with MB (100 ml, with a concentration of 10 mg L^{-1}) in a 100 ml Pyrex flask. To obtain a complete adsorption-desorption

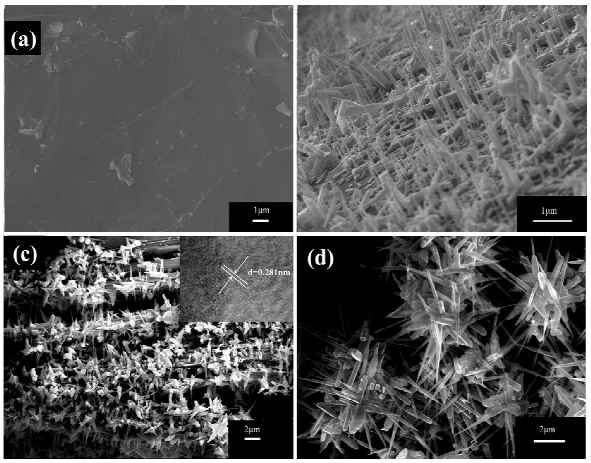

Fig. 1 SEM images of VMT surface (a); the surface (b) and edge (c) of $KNbO_3$/VMT composite, inset: HRTEM image of a needle tip of $KNbO_3$ powder; SEM images of the $KNbO_3$ powder (d).

equilibrium, the suspension was magnetically stirred in the dark for 0.5 h. Afterwards, the flask was exposed to visible light irradiation with a maximum illumination time up to 135 min. The light source was a 300 W xenon lamp located at ca. 12 cm away from the suspension surface. In the process of photocatalysis, the suspension was continuously stirred and the reaction system was placed in a cycling water bath. About 3 mL suspensions were sampled every 15 min and centrifuged the samples several times to remove the residues. The dye concentration was evaluated according to the absorbance of MB at 665 nm in step time on a UV-vis spectrophotometer (Lambda 35, PerkinElmer).

For comparison, the same amount of $KNbO_3$ powder and VMT (0.3 g, respectively) were used in the photocatalysis tests with the same process.

2.4 Scavenging experiments

The role of HO• and $O_2^{\bullet-}$ in the degradation mechanism was assessed by the addition of 2 ml i-PrOH, 1 × 10^{-3} M p-BQ, respectively. For all the experiments, 0.3 g $KNbO_3$/VMT were added into MB aqueous solution (100 mL, 10 mg/L) with or without adding the scavenger. The mixtures were magnetically stirred in the dark for 30 min before the reaction to encourage even dispersion of the composite and to establish an absorption/desorption equilibrium. The photocatalytic reaction was conducted at room temperature, with constant magnetic stirring to ensure full suspension of the composite throughout.

3. Results and discussion

3.1 Morphology and structure of samples

The morphologies of pristine VMT, $KNbO_3$/VMT hybrid and $KNbO_3$ powder are shown in Fig. 1. It is clearly to see that the surface of VMT is very smooth (Fig. 1a). After hydrothermal treatment, $KNbO_3$ needles have closely grown on the surface of VMT to show a nanoarry structure (Fig. 1b), and the length of $KNbO_3$ needles is about 2 μm. The edge SEM image of as-synthesized $KNbO_3$/VMT composite (Fig. 1c) displayed that the distance of the VMT host layers was expanded by $KNbO_3$ needles. Obviously, the $KNbO_3$ needles have grown both on the outer and inner surfaces of layered VMT which was beneficial for the loading of $KNbO_3$ on VMT. The lattice structure of $KNbO_3$ grown on VMT was further investigated by HRTEM image (the inset in Fig. 1c). It is shown that the lattice fringe spacing of the needle is about 0.281 nm, which is corresponding to the theoretical (111) crystal plane of $KNbO_3$.[3c] In contrast, the SEM image of $KNbO_3$ powder (Fig. 1d) indicates the needles present a dendritic growth mode. The length of the branch is up to 1 - 4 μm, and there is a little agglomeration.

The elemental analysis of VMT surface before and after the growth of $KNbO_3$ was done by EDX mapping testing (Fig. 2). As shown in Fig. 2a and b, there is a tiny amount of Nb (the instrument can't give the amount, nearly 0% wt) in pristine VMT. For $KNbO_3$/VMT, the Nb element is homogeneously distributed on the sample and the contents of Nb is about 26.9% wt (Fig. 2c and d). The result further indicates that

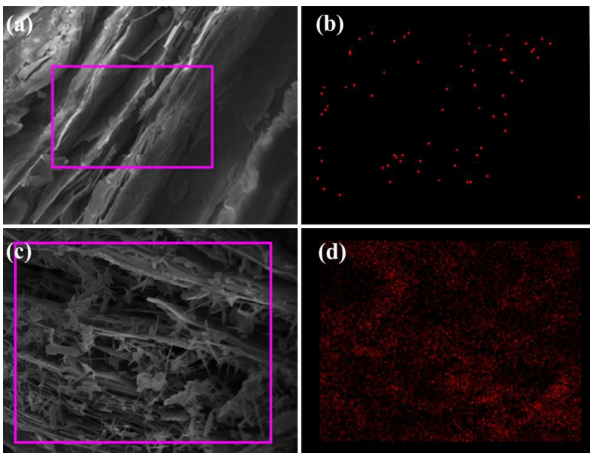

Fig. 2 SEM image of VMT (a) and $KNbO_3$/VMT (c); (b) and (d) are EDS maps of Nb in VMT and $KNbO_3$/VMT, respectively.

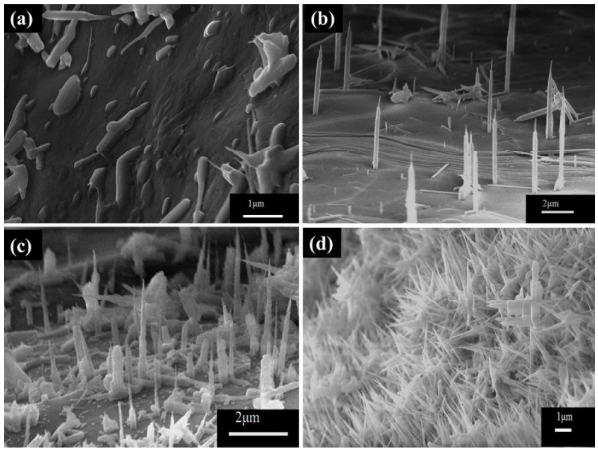

Fig.3 SEM images of $KNbO_3$/VMT samples produced with different reaction time: 8 h (a), 9 h (b), 10 h (c) and 12 h (d).

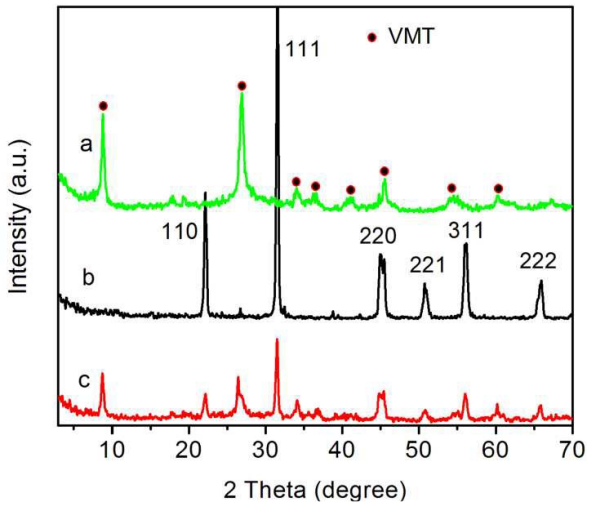

Fig. 4 XRD patterns of VMT (a), $KNbO_3$ (b) and $KNbO_3$/VMT (c).

$KNbO_3$ has *in situ* grown on the surface and interlayer of VMT by the hydrothermal route.

Fig. 3 shows the *in situ* growth process of $KNbO_3$ on VMT. At first, some irregular particles appeared on the smooth surface of VMT after the hydrothermal treatment for about 8 h (Fig. 3a). After reaction for 9 h, some needles were perpendicularly formed on the surface of VMT substrate (Fig. 3b). Thereafter, the density of the highly oriented $KNbO_3$ needles was increasing with the hydrothermal time prolonged (Fig. 3c and d). When the reaction time was extended to 12 h, a dense nanoarry of $KNbO_3$ needles was formed on all over the surface of VMT (Fig. 3d). Obviously, the mass loadings of $KNbO_3$ increased with the hydrothermal time (as is shown in Table S1). For 12 h treatment, the $KNbO_3$ loading is about 9.85 wt%.

The XRD patterns of VMT, $KNbO_3$ powder and $KNbO_3$/VMT composite are shown in Fig. 4. The XRD spectrum of VMT is consistent with the previous report (Fig. 4a).[7b] For the pristine $KNbO_3$ powder (Fig. 4b), a serious of reflections at 22.1°, 31.4°, 44.9°, 50.8°, 55.9° and 65.8°, respectively, which can be indexed as the (110), (111), (220), (221), (311) and (222) reflections of a $KNbO_3$ phase.[1a] Compared with that of VMT and $KNbO_3$, some diffraction peaks superimposed on XRD pattern of VMT substrate and $KNbO_3$ are observed in the case of $KNbO_3$/VMT composite (Fig. 4c), indicating that the $KNbO_3$/VMT composite has been fabricated by hydrothermal precipitation method.

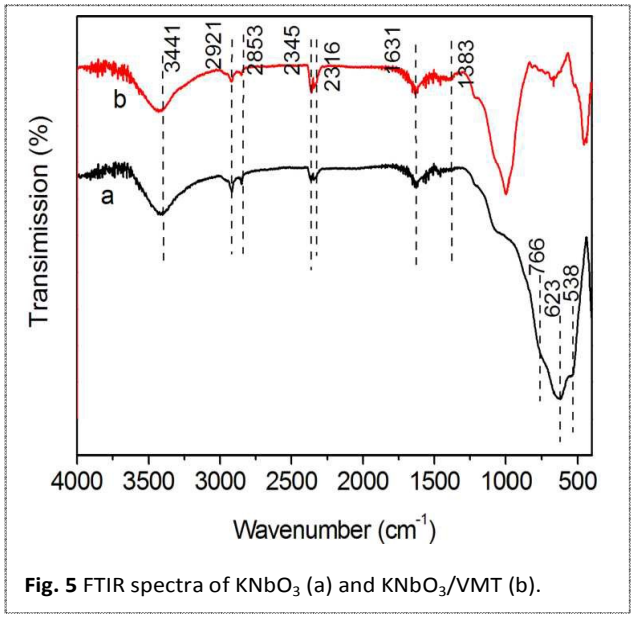

Fig. 5 FTIR spectra of $KNbO_3$ (a) and $KNbO_3$/VMT (b).

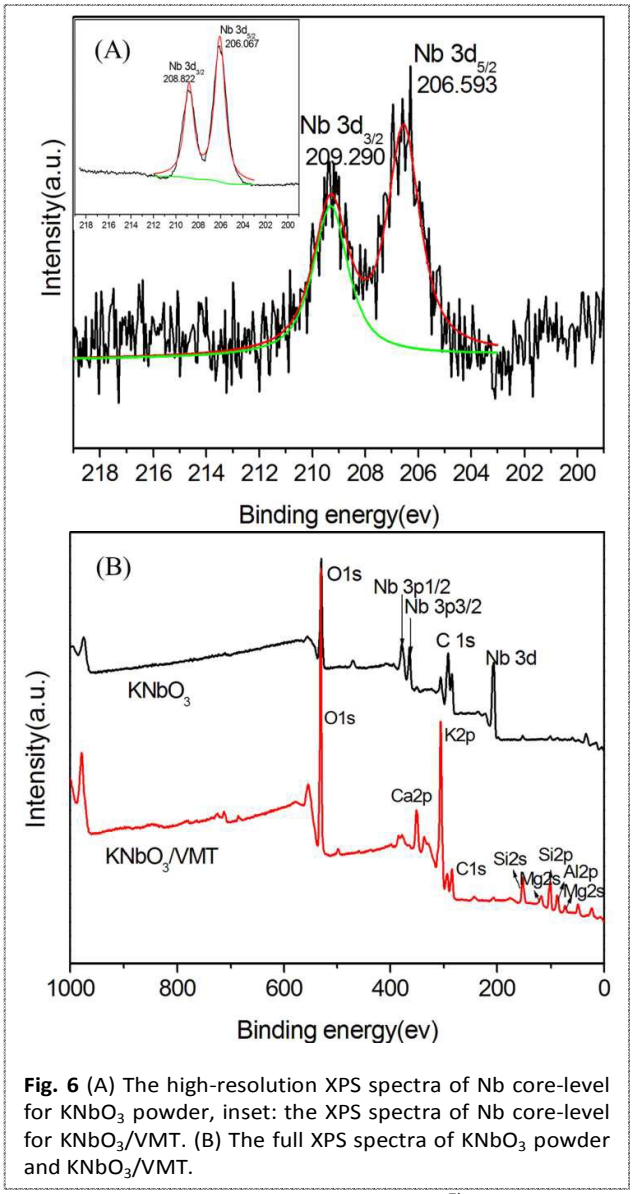

Fig. 6 (A) The high-resolution XPS spectra of Nb core-level for $KNbO_3$ powder, inset: the XPS spectra of Nb core-level for $KNbO_3$/VMT. (B) The full XPS spectra of $KNbO_3$ powder and $KNbO_3$/VMT.

On the FTIR spectrum of $KNbO_3$ powder (Fig. 5a), the absorption peaks in the range of 450-1000 cm^{-1} can be attributed to NbO_6 octahedron.[13] The band which represents O–Nb–O stretching vibration (ν_3 mode) in the corner-shared NbO_6 centered at ca. 623 cm^{-1}. The band at 538 cm^{-1} is attributed to edge-shared NbO_6 octahedron. The peaks at 3441 and 1641 cm^{-1} can be ascribed to H_2O adsorbed on the

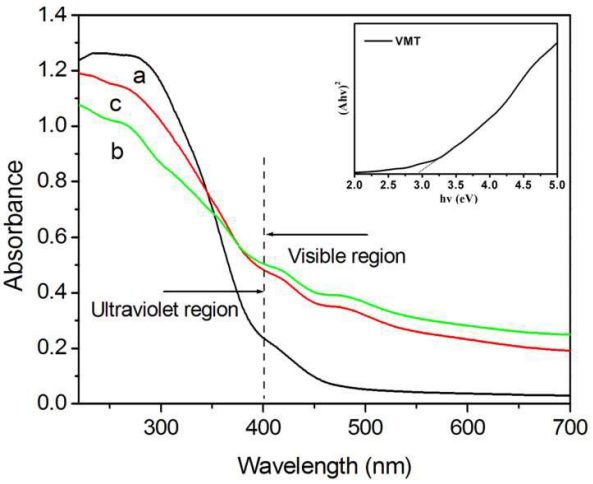

Fig. 7 DRUV-vis spectra of $KNbO_3$ (a), VMT (b) and $KNbO_3$/VMT (c).

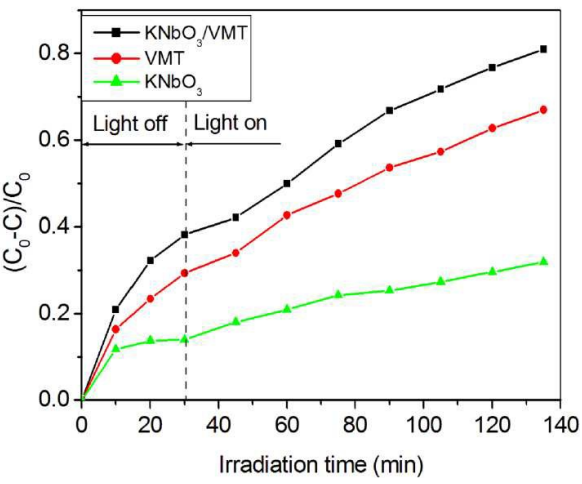

Fig. 8 Photocatalytic activity of $KNbO_3$, VMT and $KNbO_3$/VMT for MB removal under visible-light irradiation. The initial MB concentration was 10 mg/L.

surfaces of samples, and the bands corresponding to adsorbed CO_2 are presented at 2316, 2345 and 1383 cm^{-1}.[1a,13] The same peak signals appeared on the FTIR spectrum of $KNbO_3$/VMT (Fig. 5b). Both the XRD and FTIR data indicate that the $KNbO_3$ phase has been grown on the surface of VMT.

In general, a larger surface area could offer more active adsorption sites that are catalytically active, which means the higher surface area will result in the higher photocatalytic activity. N_2 adsorption/desorption isotherms were used to investigated the specific surface area of VMT, $KNbO_3$ and $KNbO_3$/VMT composite. As is shown in Table S2, after $KNbO_3$ grown on VMT, the $KNbO_3$/VMT composite acquired a larger surface area than $KNbO_3$ powder. However, after $KNbO_3$ was loaded onto VMT, the surface area of the composite decreased compared with pristine VMT. The results may indicate that $KNbO_3$ was partly occupied both the outer and inner surfaces of VMT.

The oxidation state of the as-prepared samples was revealed by high-resolution XPS (Fig. 6). The high-resolution XPS spectra of Nb3d for the $KNbO_3$ and $KNbO_3$/VMT are shown in Fig. 6A. The binding energies corresponding to $Nb3d_{5/2}$ and $Nb3d_{3/2}$ are 206.067 and 208.822 eV in $KNbO_3$, which consistent with previous study (Fig. 6A inset).[3a] However, compared with that of $KNbO_3$, the binding energy of Nb3d for $KNbO_3$/VMT is increased (Fig. 6A). The two binding energies are shift to 206.593 and 209.290 eV, respectively. The increased binding energy of $Nb3d_{5/2}$ and $Nb3d_{3/2}$ in $KNbO_3$/VMT composite can be attributed to the stronger bond (O-Nb-O) situation between VMT and $KNbO_3$ for the Nb^{5+} in $KNbO_3$/VMT composite than that of in $KNbO_3$. Fig. 6B shows a full XPS spectrum comparison of $KNbO_3$ powder and $KNbO_3$/VMT composite. The binding energies of 73.41 (Mg 2s), 87.82 (Al 2p), 101.15 (Si 2p), 530.82 (O 1s), 305.23 (K 2p), and 258.20 (C 1s) are ascribed to the Mg, Al, Si, O, K, and C elements in VMT.[11] The photoelectron peak of the C element is referred to the adventitious hydrocarbon from the XPS instrument itself. It can be observed that the $KNbO_3$/VMT composite consist not only Mg, Al, Si, O, K, and C, but also Nb element. These results are agreement with EDX analysis which further confirmed the presence of $KNbO_3$ on the VMT surface.

According to the EDX and XPS results, the *in situ* growth mechanism of $KNbO_3$ on the VMT surface can be explained as follows. The reaction processes most likely involve an "oriented absorption" and an "*in situ* growth".[14] Firstly, the Nb^{5+} is easily absorbed on the surface of VMT because of the negatively charged layer. Secondly, under a suitable temperature, the crystal seeds of $KNbO_3$ are gradually grown on the surface of VMT layer. Moreover, there is a little Nb in natural VMT, which can be functioned as seed crystals for $KNbO_3$ needles grown. Thirdly, with extended reaction time, the crystal seeds of $KNbO_3$ have been grown into $KNbO_3$ needles. The Nb element in VMT makes the possibility of $KNbO_3$ orientationally grow on the surface.

3.2 Optical absorption property and photocatalytic activity

The photophysical properties of $KNbO_3$, VMT and $KNbO_3$/VMT were revealed by RUV-vis spectroscopy (Fig. 7). The absorption of $KNbO_3$ (Fig. 7a) in the range from 400 to 700 nm is very weak, while the absorption of VMT (Fig. 7b) in this region is stronger. As for $KNbO_3$/VMT (Fig. 7c), the absorption region has been widened into the visible range. Although the absorption of VMT in visible range is stronger, it is usually used as absorbent and its photocatalytic property is very poor. The as-synthesized composite displays a relatively weaker absorption comparison with VMT in visible range, but is much stronger than that of $KNbO_3$ powder. The results indicate that the $KNbO_3$/VMT composite extended the absorption range from ultraviolet region to visible region, which benefit to enhance the utilization of sunlight in photocatalysis process. The direct band gap value of the VMT sample was estimated from the $(\alpha h\nu)^2$ *versus* photon energy ($h\nu$) plot as shown in the inset of Fig. 7. The extra polation of the linear regions in the

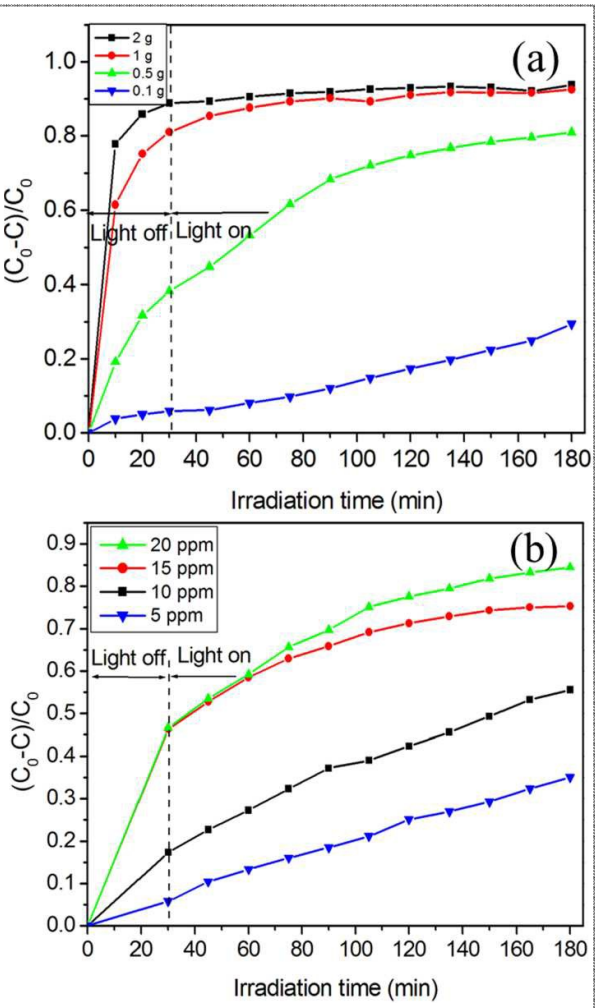

Fig. 9 (a) The different removal rate of MB in different amount of $KNbO_3$/VMT composite with initial MB concentration was 20 mg/L. (b) Removal rate versus time with various initial concentrations of MB. The amounts of catalysts were all 0.3 g.

Tauc plot suggests one-regime optical absorption by VMT, where the associated direct optical band gap is about 2.9 eV.[9] The band gap for commercial $KNbO_3$ is about 3.26 eV reported in previous study.[15]

PL spectrum testing is a well known technique to study transfer process of the interface charge carrier as well as the recombination process involving the electron-hole pairs in semiconductor particles, and PL emission results from the radiative recombination of excited electrons and holes.[16] As shown in Fig. S1, VMT displayed a strong PL intensity, meaning the high recombination of charge carriers in VMT. After the $KNbO_3$ nanoneedles grown on VMT, the PL intensity decreased, indicating that the recombination of the photogenerated electron-hole pairs is efficiently. Furthermore, the intimate and large contact interfaces with VMT have also improved the lifetime and transfer of photogenerated charge carriers.[17] Based on the PL results, the intensity of $KNbO_3$ is weaker than that of $KNbO_3$/VMT, meaning the better separation of photogenerated charge carriers. However, the efficiency of the photodegradation was lower than that of $KNbO_3$/VMT, which is probably attributed to the higher content of surface oxygen vacancies and defects of the composite.[18]

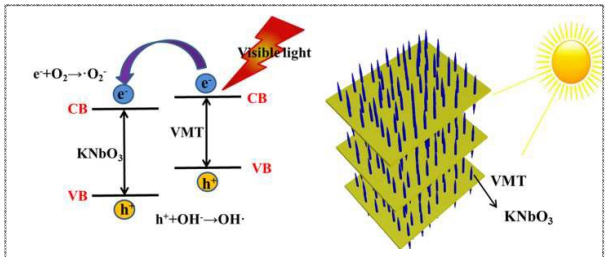

Fig. 10 The photocatalysis schematic diagram of $KNbO_3$/VMT composite.

The removal of MB under visible-light illumination was used for evaluating the photocatalytic performance of as-synthesized $KNbO_3$/VMT composite. The photocatalytic performance of $KNbO_3$, VMT and $KNbO_3$/VMT is shown in Fig. 8. Before photo-degradation experiment, the suspension including photocatalyst and MB was stirred for 30 min in the dark in order to reach a complete adsorption–desorption equilibrium. Fig. 8 shows a clearly sharp decrease of MB concentration due to absorption in the first 30 min. It is observed that the MB removal percentages on the three materials increase slowly after adsorption for 20 min, almost reaching a plateau between 20 min and 30 min, which indicates the adsorption equilibrium was achieved. The MB removal percentages on $KNbO_3$, VMT and $KNbO_3$/VMT by adsorption achieved 13.9%, 29.3% and 38.2%, respectively. MB adsorption percentages over the composite in the dark was used to calculate the equilibrium adsorption capacity of the sample. As shown in Fig. S2, it was about 2.165 mg/g. It is noticed that the MB removal percentage of the composite is larger than that of $KNbO_3$ and VMT, which may be due to the larger surface area of the $KNbO_3$/VMT that induced to the open layer structure which expanded by the growth of $KNbO_3$ needles on the inner surfaces of VMT. Subsequently, when opening the light, the removal percentage of the composite had an obvious increase caused by photocatalysis. With reaction proceed, the MB removal percentages on $KNbO_3$, VMT and $KNbO_3$/VMT achieved 32%, 67% and 81% after visible light irradiation for 105 min, respectively. The photocatalytic performance of $KNbO_3$/VMT is better than that of $KNbO_3$, which can be explained that after grown $KNbO_3$needles on the surface of VMT layers, $KNbO_3$/VMT with 3D structure supplied lots of active sites exposed to environment that can enhance the photocatalytic ability, resulting efficiently removal percentage for the dye.[15] In addition, the VMT is transparent, which is propitious to the visible light irradiates the $KNbO_3$ needles from all angles. Therefore, the $KNbO_3$ needles grown on the VMT surface can take advantage of the use of visible light. All above data suggested that the MB removal efficiency of the composite was improved by combining the synergetic effect both the high photoactivity of $KNbO_3$ and good absorption of VMT.

The effect of $KNbO_3$/VMT amount on the removal of MB is shown in Fig. 9a. Obviously, the reaction speed would be improved with an appropriate increase of the amount of catalyst. As the amount of the catalyst increased from 0.1 g to 0.5 g, the removal percentage increased from 28% to 81%. When 0.5 g catalyst was added, it almost reached reaction equilibrium after 120 min. The 0.5 g catalyst provided about 81% removal rate of MB after 150 min irradiation, while the removal rate just was only 28% with 0.1 g catalyst under the same conditions. The reason can be explained as that, with the increasing amount of catalyst, the solid-liquid interface for adsorption and catalysis was enlarged, resulting the material absorbs much more organic dyes. When the amount of catalyst was 1 g and 2 g, the strong absorption played a major role in eliminating dye molecules. After 30 min, it almost removed about 85% of MB. Furthermore, the photocatalytic ability is not fully displayed when excess amount of catalyst was added into MB solution. In addition, the effect of initial concentration of MB on the photocatalytic ability was also investigated. Fig. 9b shows the different removal rate of 3D $KNbO_3$/VMT catalyst *vs* various concentrations of MB. Obviously, the MB degradation rate was enhanced by the initial MB concentration increasing, which can be attributed to that there is much more contact probability between catalysts and MB molecules in high concentration. The recycle study was used to evaluate the stability and reusability of the materials. As shown in Fig. S3, after the third catalytic recycle, the MB removal percentage was still above 75%, indicating the composite has high stability and reusability during the recycles.

BQ (O_2•$^-$ scavenger) and i-PrOH (HO• scavenger) have been used to discern the participation of O_2•$^-$ and HO• in the photocatalysis mechanism.[19] In our experiment, the removal percentages of MB were decreased when BQ and i-PrOH were added to the photocatalytic system, respectively (Fig. S4). The results clearly show the contribution of O_2•$^-$ and HO• to MB degradation. Fig. 10 shows the photocatalysis schematic diagram of $KNbO_3$/VMT composite for the degradation of MB. Firstly, when $KNbO_3$/VMT was exposed to visible light, only the electrons in the valence band (VB) of VMT can be excited. The electrons in the conduction band (CB) of $KNbO_3$ can migrate to the CB of VMT, which leads to the separation of carriers. Secondly, the $KNbO_3$ and VMT semiconductors can generate pairs of electrons and holes under light illumination. Then the adsorbed O_2 can react with the photoelectrons to produce superoxide radical anions (O_2•$^-$). Meanwhile, the H_2O molecules can react with the holes to produce hydroxyl radicals (OH•). Both the superoxide radical anions and hydroxyl radicals are important in the degradation of organic molecules.[20] According to the cooperation effects, the $KNbO_3$/VMT composite exhibits a well degradation for MB in visible light range.

4. Conclusions

In summary, we have fabricated a 3D structured $KNbO_3$/VMT composite by an *in situ* hydrothermal method. $KNbO_3$ nanoneedles have grown vertically both on the inner and outer surfaces of layered VMT to form a nanoarry structure. Furthermore, the photocatalytic property of $KNbO_3$/VMT composite was also investigated by the degradation of MB molecule in visible light range. The removal percentage of MB can achieved 81% in 105 min with 0.3 g catalyst. $KNbO_3$/VMT with 3D structure provided lots of the active sites exposed to environment that can enhance the photocatalytic ability. Moreover, the cooperation effect of adsorption and photocatalysis occurred in the removal process. Thus, it can be concluded that the 3D structured $KNbO_3$/VMT composite has more practical applications in photocatalysis and environmental remediation.

Acknowledgements

This work was supported by the 973 Program (no. 2014CB932104), National Natural Science Foundation of China, Program for New Century Excellent Talents in Universities, Fundamental Research Funds for the Central Universities（ZZ1501 and YS1406）and Program for Changjiang Scholars, Innovative Research Team in University (no. IRT1205) and Beijing Engineering Center for Hierarchical Catalysts of P. R. China.

Notes and references

1 (a) T. Zhang, K. Zhao, J. Yu, J. Jin, Y. Qi, H. Li, X. Hou and G. Liu, *Nanoscale*, 2013, **5**, 8375; (b) M. Peña and J. L. G. Fierro, *Chem. Rev*., 2001, **101**, 1981.
2 (a) Y. Saito, H. Takao, T. Tani, T. Nonoyama, K. Takatori, T. Homma, T. Nagaya and M. Nakamura, *Nature*, 2004, **432**, 84;(b) Z. Cheng, K. Ozawa, M. Osada, A. Miyazaki and H. Kimura, *J. Am. Ceram. Soc.*, 2006, **89**, 1188; (c) Y. Nakayama, P.J. Pauzauskie, A. Radenovic, R.M. Onorato, R.J. Saykally, J. Liphardt and P. Yang, *Nature*, 2007, **447**, 1098; (d) J. Huang, Z. Chen, Z. Zhang, C. Zhu, H. He, Z. Ye, G. Qu and L. Tong, *Appl. Phys.Lett.* 2011, **98**, 093; (e) Y. Guo, K. Kakimoto and H. Ohsato, *Appl. Phys. Lett*., 2004, **85**, 4121; (f) F. Dutto, C. Raillon, K. Schenk and A. Radenovic, *Nano Lett*.,2011, **11**, 2517; (g) Q. Ding, Y. Yuan, X. Xiong, R. Li, H. Huang, Z. Li, T. Yu, Z. Zou and S. Yang, *J. Phys. Chem. C*, 2008, **112**, 18846; (h) G. Li, N. Yang, W. Wang and W. Zhang, *J. Phys. Chem. C*, 2009, **113**, 14829.
3 (a) X. Li, N.K. Kikugawa and J. Ye, *Adv. Mater.,* 2008, **20**, 3816; (b) D. Staedler, T. Magouroux, R. Hadji, C. Joulaud, J. Extermann, S. Schwung, S. Passemard, C. Kasparian, G. Clarke and M. Gerrmann, 2012, *ACS Nano*, **6**, 2542; (c) L. Jiang, Y. Qiu and Z. Yi, *J. Mater. Chem. A*, 2013, **1**, 2878.
4 J. Lan, X. Zhou, G. Liu, J. Yu, J. Zhang,L. Zhi and G. Nie, *Nanoscale*, 2011, **3**, 5161.
5 R. Wang, Y. Zhu, Y. Qiu, C. Leung, J. He, G. Liu and T. Lau, *Chem. Eng. J.*, 2013, **226**, 123.
6 X. Wang, Y. Liu, Z. Hu, Y. Chen, W. Liu and G. Zhao, *J. Hazard. Mater*, 2009, **169**, 1061.
7 (a) S. Froehner, K. S. Machado and F. Falcao, *Water Air Soil Pollut.*, 2010, **209**, 357; (b) T. Kogure, K. Morimoto, K. Tamura, H. Sato andA. Yamagishi, *Chem. Lett.*, 2012, **41**, 380.
8 Y. Qian, C. I. Lindsay, C. Macosko and A. Stein, *ACS Appl. Mater. Interfaces,* 2011, **3**, 3709.
9 J. Zhang, W. Zhu and X. Liu, *Dalton Trans*., 2014, **43**, 9296.

10 (a) X. Zhou, H. Yang, C. Wang, X. Mao, Y. Wang,Y. Yang and G. Liu, *J. Phys. Chem. C,* 2010, **114**, 17051; (b) J. Xu, Y. Meng, R. Li, Y. Xu and A. V. Rajulu, *J. Polym. Sci. B,* 2003, **41**, 749.
11 J. Lin, Q. Tang, J. Wu and H. Sun, *Sci. Technol. Adv. Mater.* 2008, **9**. 025010.
12 R. Neumann, G. E. L. Costa, J. C. Gaspar, M. Palmieri and S. E. Silva, *Miner. Eng.*, 2011, **12**, 1323.
13 J. S. d. Andrade, A. G. Pinheiro, I. F. Vasconcelos, J. M. Sasaki, J. A. C. d. Paiva, M. A. Valente and A. S. B. Sombra, *J. Phys.: Condens. Matter*, 1999, **11**, 4451.
14 (a) L. Mai, F. Yang, Y. Zhao, X. Xu, L. Xu and Y. Luo, *Nat. Commun.*, 2011, **2**, 381; (b) H. Colfen and Antonietti, M. *Angew. Chem., Int. Ed.*, 2005, **44**, 5576; (c) R. L. Penn and J. F. Banfield, *Science*, 1998, **281**, 969.
15 (a) M. R. Hoffmann, S. T. Martin, W. Choi, D. W. Bahnemann, *Chem. Rev.*,1995, **95**, 69; (b) A. L. Linsebigler, G. Lu and J.T.J. Yates, *Chem. Rev.*,1995, **95**, 735; (c) A.G.S. Prado, L.B. Bolzon, C.P. Pedroso, A.O. Moura and L.L. Costa, *Appl. Catal. B*,2008, **82**, 219; (d) J. Pan, H. Dou, Z. Xiong, C. Xu, J. Ma and X. Zhao, *J. Mater. Chem.,* 2010, **20**, 4512.
16 (a) K. K. Haldar, G. Sinha, J. Lahtinen and A. Patra, *ACS Appl. Mater. Interfaces*, 2012, **4**, 6266; (b) X. Xin, R. Liu, X. Yu, G. Zhang, H. Cao, J. Ya, B. Ren, Z. Jiang and H. Zhao, *J. Mater. Chem. A,* 2013, **1**, 1488; (c) Y. Shi, H. Li, L. Wang, W. Shen and H. Chen, *ACS Appl. Mater. Interfaces*, 2012, **4**, 4800.
17 S. Han, L. Hu, Z. Liang, S. Wageh, A. Ghamdi, Y. Chen and X. Fang, *Adv. Funct. Mater.*, 2014, **24**, 5719.
18 L. Jing, Y. Qu, B. Wang, S. Li, B. Jiang, L. Yang, W. Fu, H. Fu and J. Sun, *Sol. Energy Mater. Sol. Cells*, 2006, **90**, 1773.
19 Y. Lin, D. Li, J. Hu, G. Xiao, J. Wang, W. Li and X. Fu, *Appl. Catal. B,* 2016, **192**,152.
20 L. Pan, X. Liu, Z. Sun and C. Q. Sun, *J. Mater. Chem. A*, 2013,**1**, 8299.

Three-Dimensional Potassium Niobate Nanoarray on Vermiculite for High-performance Photocatalyst Fabricated by an in situ Hydrothermal process

Yuwei Wang, [a] Xianggui Kong, [a,*] Weiliang Tian,[a] Deqiang Lei [b] and Xiaodong Lei [a,*]

Graphical abstract:

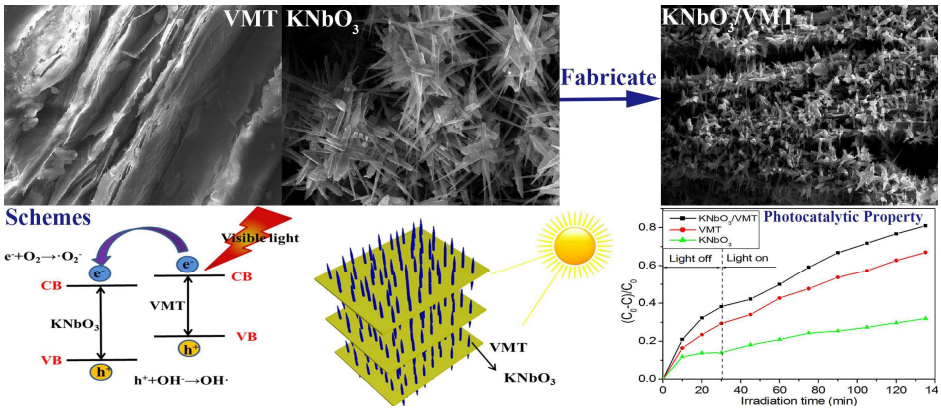

The 3D $KNbO_3$/VMT hierarchical architecture can be synthesized by a facile hydrothermal method, which shows high visible-light photocatalytic activity.